

# Enzymic characterization with progress curve analysis of a collagen peptidase from an entomopathogenic bacterium, *Photorhabdus luminescens*

Judit MAROKHÁZI\*, György KÓCZÁN†, Ferenc HUDECZ‡, László GRÁF\*, András FODOR‡ and István VENEKEI\*<sup>1</sup>

\*Department of Biochemistry, Eötvös Loránd University, Pázmány sétány 1/C, Budapest, H-1117 Hungary, †Research Group of Peptide Chemistry, Hungarian Academy of Sciences, Budapest, Hungary, and ‡Department of Genetics, Eötvös Loránd University, Pázmány sétány 1/C, Budapest, H-1117 Hungary

A proteolytic enzyme, Php-B (*Photorhabdus* protease B), was purified from the entomopathogenic bacterium, *Photorhabdus luminescens*. The enzyme is intracellular, and its molecular mass is 74 kDa. Tested on various peptide and oligopeptide substrates, Php-B hydrolysed only oligopeptides, with significant activity against bradykinin and a 2-furylacryloyl-blocked peptide, Fua-LGPA (2-furylacryloyl-Leu-Gly-Pro-Ala;  $k_{\text{cat}} = 3.6 \times 10^2 \text{ s}^{-1}$ ,  $K_m = 5.8 \times 10^{-5} \text{ M}^{-1}$ , pH optimum approx. 7.0). The  $\text{p}K_{\text{a}1}$  and the  $\text{p}K_{\text{a}2}$  values of the enzyme activity (6.1 and 7.9 respectively), as well as experiments with enzyme inhibitors and bivalent metal ions, suggest that the activity of Php-B is dependent on histidine and cysteine residues, but not on serine residues, and that it is a metalloprotease, which most probably uses  $\text{Zn}^{2+}$  as a catalytic ion. The enzyme's ability to cleave oligopeptides that contain a sequence similar to collagen repeat (-Pro-Xaa-Gly-), bradykinin and Fua-LGPA (a synthetic substrate for bacterial collagenases and collagen peptidases), but not native collagens

(types I and IV) or denatured collagen (gelatin), indicates that Php-B is probably a collagen peptidase, the first enzyme of this type to be identified in an insect pathogen, that might have a role in the nutrition of *P. luminescens* by degrading small collagen fragments. For the determination of enzyme kinetic constants, we fitted a numerically integrated Michaelis–Menten model to the experimental progress curves. Since this approach has not been used before in the characterization of proteases that are specific for the P1'–P4' substrate sites (e.g. collagenolytic enzymes), we present a comparison of this method with more conventional ones. The results confirm the reliability of the numerical integration method in the kinetic analysis of collagen-peptide-hydrolysing enzymes.

Key words: collagen peptidase, metalloprotease, numerical simulation, *Photorhabdus luminescens*, progress curve analysis.

## INTRODUCTION

Entomopathogenic bacteria from the genus *Photorhabdus* (Enterobacteriaceae) [1–3] live in symbiosis with nematodes belonging to the genus *Heterorhabditis*. The bacteria cannot infect the insect without the nematodes. They are carried in the gut of the nematodes and released into the haemocoel upon nematode invasion of the insect host. Once inside, they first overcome the insect immune response and kill the host. Then, by penetrating the tissues and converting the cadaver into a monoxenic bacterial culture, they provide the nutritional conditions that are needed for the nematode to complete several life cycles [4]. This system is an easily accessible laboratory model of symbiosis and the infection process. These bacteria are also of interest for the potential use of the symbiotic complex in the environmentally friendly biocontrol of harmful agricultural insect pests [5]. So far, the pathomechanisms of *Heterorhabditis* and *Photorhabdus* have been studied mostly at the organism and cellular levels, while investigations at the molecular level have become intensive only recently [6,7]. Thus, apart from high-molecular-mass toxin molecules [8–11], other virulence factors of *Photorhabdus* that might also be essential for the interaction with the host have not yet been identified (e.g. molecular mechanisms to survive and neutralize the defence mechanisms or to invade tissues). Secreted proteolytic enzymes can have such functions, as has been shown for several other micro-organisms [12–14]. The secretion of

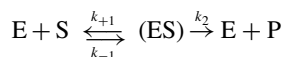
proteolytic activity by *Photorhabdus* strains has been documented previously. Some of these enzymes were partially purified, mostly from 10–15-day cultures [15–18], but they were not characterized in detail and their physiological functions remain unknown.

In order to identify proteases that might have functions in the establishment of infection, we have investigated the proteolytic activity in the culture medium of *Photorhabdus* strains using a combination of various detection methods (I. Venekei and J. Marokházi, unpublished work). We found four different proteolytic enzyme activities in the case of strain *P. luminescens* ssp. *laumondii* (str. Brecon). One of these (referred to here as Php-B, for *Photorhabdus* protease B) was detected due to its pronounced hydrolysis of Fua-LGPA (2-furylacryloyl-Leu-Gly-Pro-Ala), a synthetic substrate for bacterial collagenases and related enzymes. Here we describe the purification and characterization of this protease, which appears to be a collagen peptidase, the first of this type of protease to be isolated from an insect pathogen prokaryotic micro-organism.

For the determination of kinetic parameters, several sophisticated methods are available, which are based on the analysis of kinetic progress curves (time-dependence curves that are obtained by allowing the enzyme-catalysed reactions to proceed beyond the initial phase of the reaction). Since these use all of the information in a kinetic run, significant savings in time and reagents can be achieved compared with the more conventional initial-rate analysis. These benefits of progress curve analysis-based methods

Abbreviations used: AMC, 7-amino-4-methylcoumarin; Bu<sup>t</sup>, t-butyl; DEPC, diethyl pyrocarbonate; DMF, dimethylformamide; DTT, dithiothreitol; Fmoc, 9-fluorenylmethyloxycarbonyl; Fua, 2-furylacryloyl; Fua-LGPA, 2-furylacryloyl-Leu-Gly-Pro-Ala; LB, Luria–Bertani; Php-B, *Photorhabdus luminescens* secreted protease B; TFA, trifluoroacetic acid.

<sup>1</sup> To whom correspondence should be addressed (e-mail venekei@cerberus.elte.hu).



**Scheme 1** Michaelis–Menten model used in progress curve analysis

are especially useful in the kinetic characterization of enzymes that require substrates that are expensive and/or difficult to use in initial-rate analysis. Among these enzymes are those proteases, including collagenases, that have specific binding sites for substrate residues C-terminal to the scissile bond (typically sites P1' and P2'; notation from Schechter and Berger [19]). Since Php-B belongs to this group and since its best substrate, Fua-LGPA, has high background absorbance [20,21] that makes its utilization complicated and inconvenient in initial-rate analysis, we applied progress curve analysis. The kinetic mechanism of the Michaelis–Menten model in our analysis is shown in Scheme 1.

Progress curves can be analysed by transforming the original ( $t$ , and [P] or [S]) data pairs into [S],  $d[P]/dt$  or  $d[S]/dt$  data pairs and by fitting to the steady-state equation:

$$v = d[P]/dt = d[S]/dt = k_2[E]_T[S]/(K_m + [S]) \quad (1)$$

An alternative approach is to fit [S],  $d[P]/dt$  or  $d[S]/dt$  data pairs directly to a numerically integrated Michaelis–Menten model. If  $k_{-2} = 0$ , the model is described by the following set of differential equations:

$$d[E]/dt = -k_1[(ES)] + k_{-1}[(ES)] + k_2[(ES)] \quad (2)$$

$$d[S]/dt = -k_1[(ES)] + k_{-1}[(ES)] \quad (3)$$

$$d[(ES)]/dt = k_1[(ES)] - k_{-1}[(ES)] - k_2[(ES)] \quad (4)$$

$$d[P]/dt = k_2[(ES)] \quad (5)$$

Of the calculation methods available, we employed KINSIM and FITSIM software [22,23]. During simulation of the Michaelis–Menten model, KINSIM generates pseudo experimental curves by numerical integration of equations (2)–(5) and introducing random error. FITSIM numerically compares the pseudo-experimental curves with the experimental curve(s) by calculating the summation of the squared differences between the two as a measure of goodness of fit. The two programs run in co-operation such that FITSIM adjusts the simulation parameters during repeated runs of KINSIM in accordance with an error minimization algorithm. With this procedure it is possible to find a single set of rate constants that describes the kinetics of an experiment or series of experiments [22]. The benefits of numerical integration methods are: (i) a unique solution for  $k_2$  ( $k_{cat}$ ) and  $K_m$ , (ii) information about product inhibition, and (iii) curve analysis even when substrate concentration is lower than the  $K_m$  [24].

Since, to our knowledge, this is the first time that progress curve analysis has been used in the kinetic characterization of a P1'–P4'-specific collagen-peptide-hydrolysing enzyme, we have carried out comparisons with other calculation methods, i.e. initial-rate analysis and fitting to first-order kinetics. These confirmed the parameter values obtained with the progress curve analysis.

## EXPERIMENTAL

### Substrates

Fua-LGPA and protected amino acids for the synthesis of other Fua-blocked peptide substrates were purchased from

Bachem, Bubendorf, Switzerland (all amino acids except glycine were in the L-configuration), *p*-(benzyloxy)benzyl alcohol resin and solvents were from Reanal (Budapest, Hungary), and all other reagents used in peptide synthesis were from Fluka. Des-Arg<sup>1</sup>-bradykinin, insulin B-chain and collagen types I and IV were products of Sigma-Aldrich. The AMC (7-amino-4-methylcoumarin) oligopeptide substrates were synthesized as described in [25]. Oligopeptides P065 (KTEVSSVS) and P290 [(PPG)<sub>6</sub>] were kindly provided by A. Patthy (Biotechnological Research Group, Hungarian Academy of Sciences).

Fua-blocked peptide substrates were prepared by solid-phase peptide synthesis on *p*-(benzyloxy)benzyl alcohol resin (0.3 mmol/g of resin) using an Fmoc (9-fluorenylmethoxycarbonyl)/Bu<sup>t</sup> (t-butyl) strategy. The side chain of tyrosine residues was protected as a Bu<sup>t</sup> ether, while the  $\gamma$ -carboxylic group of glutamic acid was protected as a Bu<sup>t</sup> ester. The first amino acid [3 equiv. (mol/mol) relative to resin capacity] was coupled to the solid support with the aid of *N,N'*-dicyclohexylcarbodi-imide (3 equiv.) and 4-(dimethylamino)pyridine (0.5 equiv.) using a dichloromethane/DMF (dimethylformamide) mixture (1:2, v/v). After coupling (3 h), the resin was washed thoroughly with dichloromethane and ethyl alcohol, and the coupling was repeated. After the second coupling, the resin capacity was determined using a quantitative ninhydrin assay [26], and was found to be 0.17 mmol/g for Fmoc-Tyr(Bu<sup>t</sup>)-resin and 0.22 mmol/g for Fmoc-Glu(OBu<sup>t</sup>)-resin. The N<sup>ε</sup>-protecting group was removed with 20% (v/v) piperidine in DMF. The resin then was washed with DMF, methyl alcohol (four times) and DMF (three times). The coupling of further amino acid residues as well as furylacrylic acid (3 equiv.) was performed with di-isopropylcarbodi-imide (3 equiv.) in the presence of 1-hydroxybenzotriazole (3.3 equiv.) in DMF for 1.5 h. After washing (once with DMF, three times with methanol and twice with DMF), coupling efficacy was monitored using a ninhydrin assay [26]. Fua-peptides were deprotected and cleaved from the resin with ice-cold TFA (trifluoroacetic acid) containing 5% (v/v) water as scavenger for 90 min. After cleavage, the resin was filtered out and was washed with TFA. The TFA washings were pooled, and concentrated *in vacuo*. The crude peptide was precipitated with di-isopropyl ether, and isolated by centrifugation (14000 rev./min for 2 min in an Eppendorf centrifuge). The peptide samples were dissolved in glacial acetic acid and isolated by freeze-drying.

### Purification by reverse-phase-HPLC and MS analysis of the synthesized peptide substrates

Purification of the Fua-peptides was achieved on a Jupiter C18 column (10 mm × 250 mm, 10  $\mu$ m, 300 Å pore size; Phenomenex). A linear gradient was developed from 20% to 80% eluent B in 25 min, where eluent A was 0.1% TFA in water and eluent B was 0.1% TFA in acetonitrile/water (80:20, v/v). Chromatography was carried out at a flow rate of 5.0 ml/min, at ambient temperature using UV detection at 280 nm. Fractions between 17.5 and 18.5 min (Fua-ALVE) or between 19.5 and 20.5 min (Fua-ALVY) were collected, and peptides were isolated by freeze-drying. The yield was 60% in both cases.

The purity of the peptides was checked by analytical reverse-phase HPLC using a Synergi MAX RP C12 column (4.6 mm × 250 mm, 480 Å pore size, 4.0  $\mu$ m; Phenomenex) with gradient elution from 10% to 100% eluent B in 25 min. The flow rate was 1 ml/min and peaks were detected at 280 nm. The retention time for Fua-ALVY was 20.9 min and that for Fua-ALVE was 19.5 min. Based on area under the curve values, the purity of both preparations was >95%. Matrix-assisted laser-desorption/ion

ionization spectra were acquired on a Voyager DE-Pro MALDI-TOF instrument. An  $\alpha$ -cyano-4-hydroxycinnamic acid matrix was used, and the samples were dissolved in acetonitrile/water (1:1, v/v) containing 0.1% TFA. A 0.5  $\mu$ l aliquot of saturated matrix solution was mixed with 0.5  $\mu$ l of sample solution on the target, and allowed to dry in air. Spectra were acquired in reflectron mode.

### Bacterium strain and culturing

*P. luminescens* ssp. *laumondii* strain *Brecon* cultures were grown in LB (Luria–Bertani) medium at 30 °C in a rotary shaker without antibiotics. Cultures were started as a 500 ml cell suspension of  $D_{600} \sim 0.01$  by infecting the medium with 10–15 bacterial colonies from LB plates, and then diluted to 2 litres.

### Enzymes

The 74 kDa peptidase Php-B was prepared from the supernatant of a 2 litre, early-stationary-phase (22–24 h) *Photobacterium luminescens* ssp. *laumondii* *Brecon* culture ( $D_{600} \sim 6.0$ ). The first purification step was anion-exchange chromatography on QAE-Sephadex A-50 resin (Pharmacia) at pH 8.5. After setting the pH of the culture supernatant using NaOH, binding to the resin was performed batchwise in two steps. First, 120 ml of resin was added, and after shaking for 3 h at room temperature it was filtered off. Then the procedure was repeated with the addition of 60 ml of resin to the filtrate. The two resin fractions were combined and washed three times with 600 ml of starting buffer (50 mM Tris/HCl, pH 8.5, 10 mM CaCl<sub>2</sub> and 50 mM NaCl). Then, to elute the enzyme active against Fua-LGPA, the resin was resuspended in 220 ml of starting buffer containing 1.0 M NaCl and was left to stand overnight at 4 °C. The eluate was obtained after pouring the resin into a column, which was washed with one column volume of buffer containing 1.0 M NaCl. The eluate ( $\sim 220$  ml) was concentrated first to 35 ml in an Amicon Concentrator, then by fractionated ammonium sulphate precipitation in steps of 15% and 50%. The 50% precipitate was dissolved in 7.5 ml of Tris/HCl buffer (20 mM, pH 8.0) containing 0.1 M NaCl and dialysed overnight against the same solution also containing 10 mM CaCl<sub>2</sub>. After sedimentation of the insoluble material, the clear supernatant was gel-filtered on a Sephadex G-100 (Pharmacia) column (100 cm  $\times$  1.6 cm) in the buffer used for dialysis, at a flow rate of 0.5 ml/min. The greatest activity against Fua-LGPA corresponded to the presence of a 74 kDa protein band detected by SDS/PAGE. Fractions with the highest activity were subjected to anion-exchange chromatography on a Matrex Silica PEI300 (Millipore) column (9.0 cm  $\times$  1.0 cm, equilibrated with 20 mM Tris/HCl buffer, pH 8.0, containing 10 mM CaCl<sub>2</sub> and 10 mM NaCl), using a 10–500 mM NaCl gradient. The fractions containing activity against Fua-LGPA were combined and concentrated to 1.5 ml using a Centricon (Millipore) concentrator. The final purification step was on a HiPrep 16/60 Sephacryl S-200 HR (Amersham Biosciences) gel filtration column in 20 mM Tris/HCl buffer (pH 8.0) containing 10 mM CaCl<sub>2</sub> and 150 mM NaCl. The enzyme activity was in the single protein peak that eluted from the column.

To monitor purification and to determine the size of Php-B, standard SDS/PAGE was carried out in 10% (w/v) polyacrylamide slab gels. When reducing conditions were used, the samples were heated for 5 min in the presence of DTT (dithiothreitol). The gels were stained with Coomassie Brilliant Blue R-250.

The protein concentration of the purified enzyme was determined according to Bradford.

Cell lysates were prepared from cultures at early stationary phase ( $D_{600} \sim 6$ ), similar to the culture that was used for Php-B purification. A 1 ml sample of cell suspension was pelleted, washed twice in 1.5 ml of LB broth and resuspended in 200  $\mu$ l of 0.1 M Tris buffer, pH 8.0, containing 20% (w/v) sucrose. After incubating on ice for 10 min, the suspension was centrifuged (14000 rev./min for 2 min in an Eppendorf centrifuge), the supernatant was discarded and the cells were resuspended in 1 ml of distilled water. Enzyme activity was measured after allowing cell lysis on ice for 2 h.

### Hydrolysis of non-chromogenic peptides

Peptide digestion by Php-B was carried out at 30 °C in 50 mM Mops buffer (pH 7.0) in the presence of 10 mM CaCl<sub>2</sub> and 0.1 M NaCl, at 32 nM enzyme and 0.2 mM substrate concentrations. The reactions were stopped by the addition of acetic acid to 1 M final concentration, and the cleavage products were analysed by reverse-phase HPLC. Aliquots of 24  $\mu$ l of each reaction mixture, containing 4 nmol of peptide substrate, were loaded on to a Zorbax 300 SB C-18 (4.6 mm  $\times$  25 mm) column and eluted with a linear 0–30% (v/v) acetonitrile gradient (1%/min) in 0.1% TFA, at a flow rate of 1 ml/min. The peptides in the effluent were detected at 220 nm. Percentage cleavage was calculated from peak areas.

### Enzyme activity measurements

Activity measurements were carried out at 30 °C. The standard assay buffer contained 50 mM Mops (pH 7.0), 10 mM CaCl<sub>2</sub>, 100 mM NaCl and 0.05 mg/ml BSA. The reaction was started by the addition of the enzyme, except for the enzyme inhibition and metal ion complementation experiments.

The hydrolysis of Fua-blocked peptides was monitored in a Shimadzu UV-2110PC UV–visible scanning spectrophotometer by following the decrease in light absorption at 324 nm. For progress curve analysis, the exact initial substrate concentrations, as well as the molar absorption coefficients of both the substrate and the product at 324 nm, were required. The initial substrate concentration ( $A_0$ ) was calculated from the absorbance of the reaction mixture at 305 nm at  $t = 0$  using a molar absorption coefficient of 24700 M<sup>-1</sup> · cm<sup>-1</sup> [21]. The absorption coefficients for the substrate and the product at 324 nm were measured to be 14170 M<sup>-1</sup> · cm<sup>-1</sup> and 11660 M<sup>-1</sup> · cm<sup>-1</sup> respectively. Three combinations of substrate and Php-B concentrations were used for determination of the kinetic constants with Fua-LGPA using progress curve analysis: 60  $\mu$ M and 2.25 nM, 60  $\mu$ M and 4.5 nM, and 50  $\mu$ M and 2.25 nM respectively. For determination of the kinetic constants with Fua-Ala-Leu-Val and Fua-Ala-Leu-Val-Tyr as substrates using progress curve analysis, three substrate/enzyme concentration pairs were used: 50  $\mu$ M and 2.0 nM, 25  $\mu$ M and 2.9 nM, and 50  $\mu$ M and 4.0 nM. Activity measurements for saturation kinetics with Fua-LGPA were carried out at concentrations of 1.5 nM enzyme, and 3.2, 7.0, 13.6, 27.0, 56.0 and 130  $\mu$ M substrate.

pH-dependence measurements were performed in the presence of 13.0 nM Php-B and 74  $\mu$ M Fua-LGPA. The following buffers were used: sodium acetate (pH 4.5, 5.0 and 5.5), Mes (pH 6.0 and 6.5), Mops (pH 7.0 and 7.5), Hepes (pH 8.0), Tris (pH 8.5 and 9.0) and Caps (pH 10.0).

In order to determine the effects of inhibitors, 2.0 nM Php-B was incubated with the inhibitors in 1.0 ml of standard assay buffer (above) for 20 min at room temperature, then the enzyme

reaction was started by the addition of Fua-LGPA to 60  $\mu\text{M}$  final concentration. In metal ion complementation experiments 2.0 nM Php-B was preincubated with 1.0 mM EDTA, DTT or cysteine at room temperature for 5 min in the standard assay buffer, in a final volume of 1.0 ml. Then metal ions were added to 1.5 mM final concentration, and the enzyme reaction was started after further incubation for 5 min by the addition of Fua-LGPA to 60  $\mu\text{M}$  final concentration.

The effects of DEPC (diethyl pyrocarbonate), a histidine reagent, on the activity of Php-B against Fua-LGPA was investigated by incubating 64 nM enzyme with 5 mM DEPC in 100  $\mu\text{l}$  final volume of a 0.1 M Mes (pH 6.5) buffer. After 30 min at room temperature, 100  $\mu\text{l}$  of 10 $\times$  assay buffer without BSA (see above) and 100  $\mu\text{l}$  of 0.5 mg/ml BSA were added, and the solution was dialysed for 1 h against 1.5 litres of buffer solution containing 50 mM Mops (pH 7.0), 10 mM  $\text{CaCl}_2$  and 100 mM NaCl. To measure enzyme activity, the dialysed solution was added to 700  $\mu\text{l}$  of standard assay buffer which contained 61  $\mu\text{M}$  substrate (6.4 nM enzyme and 43  $\mu\text{M}$  Fua-LGPA, final concentrations). To test the effect of the substrate on the inhibition by DEPC, Fua-LGPA (1.5 mM) was added to the reaction mixture during treatment with DEPC. The control was treated in the same way, but neither DEPC nor Fua-LGPA was added.

Activity against succinyl-Ala-Ala-Pro-Xaa-AMC substrates (Xaa = P1 = Phe, Ala or Lys) was measured at concentrations of 15 nM enzyme and 25, 50, 100, 200 and 400  $\mu\text{M}$  substrate in the standard assay buffer in a Spex Fluoromax<sup>TM</sup> Spectrofluorimeter using 380 nm excitation and 460 nm emission wavelengths.

### Calculation of kinetic constants and $\text{p}K_a$ values

In progress curve analysis, the KINSIM [22] and FITSIM [23] software packages were used to calculate the kinetic constants. During analysis, the former is run as the subroutine of the latter to generate simulated curves according to Scheme 1 with the appropriate rate constants in eqns (2)–(5). FITSIM statistically tests the fit of the simulated curve to the experimental one(s) and, after adjusting the simulation parameters in accordance with an error-minimizing algorithm, initiates a new simulation run of KINSIM. When the comparison of the pseudo experimental curve of the last model with the experimental one(s) gives no further decrease in the summation of the squared differences, the curves and the rate constants of the last simulation are displayed together with several fitted parameter values (e.g. the approximate standard error parameter was below 20% for the best fits). Since in non-regression procedures the final fit is not always the best one, runs of KINSIM/FITSIM were repeated, as the authors of the method recommended [23], with different starting values of the kinetic constants. In the Michaelis–Menten model depicted in Scheme 1, the rate constants, that were the independent variables in the course of the simulation, are related according to the equation  $K_m = (k_{-1} + k_2)/k_1$ . In order to obtain reliable values for  $k_{\text{cat}}$  and  $K_m$ , we performed analysis of five experimental curves, which were recorded under three different experimental conditions with respect to both substrate and enzyme concentrations (see above). (The minimal number of recommended curves was three in our case, because the number of varied parameters was two.)

For the correct application of progress curve analysis, knowledge of the proper kinetic scheme is needed. For Php-B and Fua-LGPA, we used Scheme 1, assuming that there is no product inhibition {i.e.  $k_{-2} \sim 0$ ,  $[(\text{EP})] \sim 0$  and  $k_2 = k_{\text{cat}}$ }. This assumption was justified by the good agreement between the  $k_2$  ( $k_{\text{cat}}$ ) and  $K_m$  values obtained from progress curve and initial-rate analysis (see Results), and by the independence of  $K_m$  and  $k_2$  values of the initial substrate concentration (results not shown).

The accurate fitting of experimental curves is dependent on the accuracy of the time parameter. Since the manual mixing during the measurements of activity with Fua-LGPA as substrate led to deviations of the time parameter associated with the mixing time, a correction of all time co-ordinates was needed. Therefore, to recalculate the time co-ordinates before progress curve analysis, we determined the actual zero time using the formula  $dt = [\ln(A_0' - A_\infty) - \ln(A_0 - A_\infty)]/k_{\text{obs}}$ , where  $A_0$  is the absorbance at  $t = 0$  (calculated from the absorbance before the addition of Php-B; see above),  $A_\infty$  is the absorbance when the enzyme reaction is complete (only the product is present),  $A_0'$  is the first absorbance measured after the addition of the enzyme, and  $k_{\text{obs}}$  was obtained by fitting the data to the normal exponential decay equation (see below). Note that at any time between  $t_0$  and complete hydrolysis, the measured absorbance is the sum of those of the substrate and the Fua-amino acid cleavage product.

For saturation kinetics, initial reaction rates were measured at different substrate concentrations (see above). The absorbance change during Fua-LGPA hydrolysis in the low concentration range was hard to detect because of the high noise-to-signal ratio, but it was assumed to be linear up to 10% of the total absorbance change. The kinetic constants  $K_m$  and  $k_{\text{cat}}$  were calculated from the initial rates using Enzfitter 1.05 software (Elsevier-Biosoft).

To examine the effects of pH, inhibitors and metal ions, first-order reaction rates ( $k_{\text{obs}}$ ) were determined using Origin 5.0 software (Microcal). They were calculated from the final portion of the time-dependence curves where, according to the absorbance, the condition  $[S] \ll K_m$  was satisfied.  $k_{\text{obs}}$  was obtained as the slope of time-dependence curves linearized using the formula  $\ln[(A_t - A_\infty)/2510]$  (where  $A_t$  is the absorbance at time  $t$ ), i.e. by fitting the data to the normal decay equation (2510 is the difference between the absorption coefficients of the substrate and the Fua-amino acid product). This method was also employed in the case of the Fua-Ala-Leu-Val-Tyr and Fua-Ala-Leu-Val substrates, where the progress curves were obtained at concentrations well below the  $K_m$ . Dividing  $k_{\text{obs}}$  values by the enzyme concentration gave the  $k_{\text{cat}}/K_m$  values.

The pH optimum and the  $\text{p}K_{a1}$  and  $\text{p}K_{a2}$  values were determined by fitting a bell-shaped curve to data points with Origin 5.0 software using the formula  $a \times \{1/[1 + \exp(-\text{pH})/\exp(-\text{p}K_{a1})]\} \times \{1/[1 + \exp(-\text{p}K_{a2})/\exp(-\text{pH})]\}$  (where  $a$  is an amplitude parameter).

## RESULTS AND DISCUSSION

### Enzyme isolation

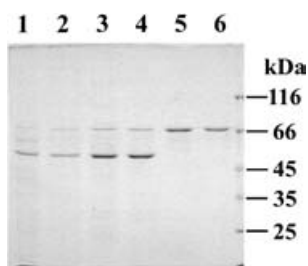
The production of Fua-LGPA peptidase activity could be detected in the bacterium culture from the early stationary phase ( $\sim 22$  h incubation;  $D_{600} \sim 6.0$ ), and it increased continuously during the stationary phase (until 62 h, the end of the culture period; results not shown). When the activities in the culture medium and cell lysate were compared, the latter proved to be 7-fold higher. Since bacterium cells do not accumulate secreted enzymes in the cytosol, this activity difference shows that the enzyme is intracellular and that it is detectable in the culture medium probably because of cell lysis. To take advantage of the low protein concentration in the culture medium, Php-B was isolated from there and not from the cell lysate. The purification was started from the 22–24 h culture, because at this time the production of a mixture of multivalent compounds (glycocalyx) of molecular masses from 10 to 10<sup>4</sup> kDa was still moderate, so that it was difficult but not impossible to achieve an acceptable yield. Table 1 summarizes the purification steps and the development of specific activity during purification, and Figure 1 shows SDS/PAGE

**Table 1** Purification of Php-B from *P. luminescens* culture

Enzyme activities are expressed as first-order rate constants ( $k_{\text{obs}}$ ), which were determined by curve fitting with Origin 5.0 software on time-dependence curves of Fua-LGPA hydrolysis.

Purification step	Volume (ml)	Protein (mg)	Total activity ( $\text{s}^{-1}$ )	Specific activity ( $\text{s}^{-1} \cdot \text{mg}^{-1}$ )	Purification (fold)	Yield (%)
1. Culture supernatant	2000	64	62	1.0	1	–
2. QAE eluate	220	17.6	128*	7.3	7.3	100
3. After $(\text{NH}_4)_2\text{SO}_4$ fractionation	7.5	20.8	103	5.0	0.7	80
4. After gel filtration	28	5.3	49	9.3	1.9	38
5. After PEI chromatography	1.2	0.18	9.5	52.8	5.7	7.4
6. After HiPrep gel filtration	5	0.10	6.1	61.0	1.2	4.8

\*The origin of the increase in total activity is unknown, but it might be attributed to the removal of inhibitors(s) of the enzyme reaction.

**Figure 1** SDS/PAGE analysis of the various purification steps

The loaded samples from each purification step contained 0.5  $\mu\text{g}$  of protein. The samples were reduced with DTT. The loadings were as follows: lane 1, culture supernatant; lane 2, QAE eluate; lane 3, 50%  $(\text{NH}_4)_2\text{SO}_4$  precipitate; lane 4, after Sephadex G-200 chromatography; lane 5, after PEI [poly(ethyleneimine)] chromatography; lane 6, after HiPrep Sephacryl S-200 gel filtration.

analysis after each purification step. Only a single protein band, the Fua-LGPA peptidase Php-B, was visible after the last step. From its mobility relative to markers, a molecular mass of 74 kDa was calculated. The absence of DTT did not influence mobility (results not shown), so either the molecule does not contain disulphide bridges or their reduction does not change the hydrodynamic size of the molecule. Comparison of the retention time of Php-B on a HiPrep S-200 gel filtration column with those of known proteins confirmed a molecular mass of 74 kDa and indicated that the active enzyme is monomer (results not shown).

### Kinetic characterization of Php-B with chromogenic substrates

Of the peptide substrates tested, those blocked at the N-terminus with the chromophore Fua group were hydrolysed efficiently by Php-B. Substrates that contained the chromophore group C-terminal to the scissile bond (at the P1' site, as in the widely used peptidyl and oligopeptide methyl coumarins or p-nitroanilides; see Table 2) were not cleaved. In the Fua-blocked peptides, the Fua group is attached to the N-terminus of the amino acid in the P1 position. When these peptides are hydrolysed at the peptide bond C-terminal to the Fua-amino acid, i.e. between the P1 and P1' sites, the charge on the liberated carboxyl group rearranges the double bond system in the Fua group. This causes a blue shift of the absorption spectrum that produces a decrease in light absorption [20,21,27]. For technical reasons, determination of the kinetic constants  $k_{\text{cat}}$  and  $K_{\text{m}}$  using such substrates might require measurements at different wavelengths to record substrate hydrolysis in concentration ranges both below and above the  $K_{\text{m}}$  [20,21]. Analysis of time-dependence curves, as an alternative, avoids this complication and, at the same time, is faster and requires much less substrate. Time-dependence

curves of collagenases and collagen peptidases have been fitted according to the normal exponential decay equation ([20,21]; see the Experimental section), which gives  $k_{\text{cat}}$  and if  $[\text{S}] \ll K_{\text{m}}$ , then  $k_{\text{cat}}/K_{\text{m}}$  can be calculated. However, to establish further properties of the enzyme reaction, such as a value for  $K_{\text{m}}$  or possible product inhibition, a more sophisticated procedure is necessary, which combines curve fitting and simulation of the enzyme mechanism by differential equations. For the characterization of Php-B, we used methods described by Barshop et al. (KINSIM; [22]) and Zimmerle and Frieden (FITSIM; [23]), which are based on numerical integration (for further details, see the Introduction and Experimental sections). Since numerical integration of kinetic progress curves has not been used previously in the kinetic analysis of proteases for which specific binding sites for P1'–P4' substrate residues are also essential, i.e. that can typically be measured with Fua-blocked peptide substrates, a validation of the method was necessary. Therefore we also calculated kinetic parameters using two other methods: by fitting time-dependence curves according to first-order kinetics, and by performing initial-rate analysis.

During measurements using Fua-LGPA (the best substrate), the high enzyme activity as well as the small change in absorbance during the reaction precluded measurements under conditions where  $[\text{S}] \ll K_{\text{m}}$ . At such a low value of  $[\text{S}]$  the reaction took place during mixing time, or – if less enzyme was added – the total absorbance change and the signal-to-noise ratio were too small. However, the evaluation of progress curves with KINSIM and FITSIM avoids these difficulties (see Introduction), demonstrating an advantage of using a simulation method based on numerical integration other than the possibility of obtaining  $k_{\text{cat}}$  and  $K_{\text{m}}$  values themselves. When the rate constant and specific activity were calculated by fitting to first-order kinetics, for the above reasons we used the final portion of progress curves (starting at  $[\text{S}] \geq K_{\text{m}}$ ), where  $[\text{S}] \ll K_{\text{m}}$ .

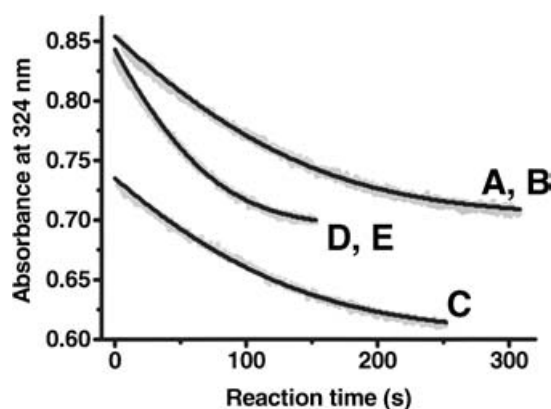
Table 2 summarizes the kinetic constants of Php-B, while Figure 2 shows the superposition of simulated curves, calculated with the FITSIM parameters in Table 2, with five experimental progress curves that were recorded under three different reaction conditions. The various determinations of kinetic constants gave values for  $k_{\text{cat}}$ ,  $K_{\text{m}}$  and  $k_{\text{cat}}/K_{\text{m}}$  that were in good agreement with each other and compared well with those of collagenases and collagen peptidases obtained using Fua-LGPA as substrate ( $k_{\text{cat}}/K_{\text{m}} \sim 5 \text{ s}^{-1} \cdot \text{M}^{-1}$ ; [21,28]).

A comparison with other chromogenic substrates showed that Php-B was by far the most active on Fua-LGPA, a substrate that mimics the collagen repeat sequence -Pro-Xaa-Gly-Pro- (where Xaa can be almost any amino acid), such that the Fua group, a proline analogue, is in the P2 substrate position. The activity was 2–3 orders of magnitude smaller, due to decreases in both catalytic efficiency ( $k_{\text{cat}}$ ) and substrate affinity (increase

**Table 2 Kinetic constants of Php-B activity on several Fua and AMC oligopeptide substrates**

Methods of calculation were as follows: A, saturation kinetics; B, progress curve analysis with KINSIM and FITSIM software; C, fitting to time-dependence curves according to first-order kinetics with Origin 5.0 software. Succ, succinyl; ND, not detectable; TL, too low for analysis.

Substrates							Method of calculation	$k_{cat}$ (s <sup>-1</sup> )	$K_m$ (M <sup>-1</sup> )	$k_{cat}/K_m$ (s <sup>-1</sup> · M <sup>-1</sup> )
P4	P3	P2	P1	P1'	P2'	P3'				
		Fua	Leu	Gly	Pro	Ala (Fua-LGPA)	A	$(2.3 \pm 0.1) \times 10^2$	$(2.6 \pm 0.4) \times 10^{-5}$	$8.6 \times 10^6$
							B	$(3.6 \pm 0.03) \times 10^2$	$(5.8 \pm 0.9) \times 10^{-5}$	$6.2 \times 10^6$
							C	–	–	$6.9 \times 10^6$
		Fua	Ala	Leu	Val	Tyr	B	$(2.8 \pm 0.8) \times 10^1$	$9.0 \times 10^{-4}$	$3.1 \times 10^4$
							C	–	–	$2.4 \times 10^4$
		Fua	Ala	Leu	Val	Glu				TL
		Fua	Ala	Leu	Val		B	$4.6 \pm 0.2$	$(1.0 \times 10^{-4})$	$4.6 \times 10^4$
							C	–	–	$2.9 \times 10^4$
		Fua	Gly	Ala	Leu					TL
Succ-Ala	Ala	Pro	Phe	AMC						ND
Succ-Ala	Ala	Pro	Lys	AMC						ND
Succ-Ala	Ala	Pro	Ala	AMC						ND

**Figure 2 Curve fitting with KINSIM and FITSIM software of the progress curves of Fua-LGPA hydrolysis by Php-B at various enzyme and substrate concentrations**

The figure shows the superposition of three simulated curves (black) on five experimental curves (A–E; grey) that were recorded under the following conditions: A and B, 2.25 nM enzyme and 60  $\mu$ M substrate; C, 2.25 nM enzyme and 50  $\mu$ M substrate; D and E, 4.5 nM enzyme and 60  $\mu$ M substrate.

in  $K_m$ ), upon loss of the substrate's collagen repeat character (e.g. P1' is not Gly and P2' is not Pro). This observation suggests that Php-B might be a collagenase or a collagen peptidase. Because of the limited number of variants in our Fua-blocked substrate set (which was designed to detect and investigate *Photorhabdus* proteases of various specificities), no conclusion can be drawn about the P1–P3' residue preferences of Php-B. However, the almost undetectable activities with Fua-Gly-Ala-Leu and Fua-Ala-Leu-Val-Glu indicate that a Gly at P1 and a negatively charged residue at P3' are particularly unfavourable for the enzyme reaction. Php-B was completely inactive on the AMC substrates listed in Table 2, which represent the three major P1 site preference types of the serine proteases trypsin, chymotrypsin and elastase respectively.

### Enzymic characterization of Php-B using inhibitors

To establish which group of proteases Php-B belongs to, the effects of several inhibitors on the Fua-LGPA-cleaving activity of the enzyme were tested (Table 3). The activity was insensitive

**Table 3 Inhibitor sensitivity and metal ion dependence of Fua-LGPA hydrolysis by Php-B**

First-order rate constants ( $k_{obs}$ ) were determined by curve fitting of time-dependence curves with Origin 5.0 software, as described in the Experimental section. For the details of inhibition conditions, see the Experimental section. Except where indicated (\*), enzyme activities were measured at concentrations of 2.0 nM enzyme and 60  $\mu$ M Fua-LGPA; 100% activity ( $k_{obs}$ ) was  $7.2 \times 10^{-3}$  s<sup>-1</sup>. \*Enzyme activities were measured at concentrations of 6.4 nM enzyme and 43  $\mu$ M Fua-LGPA; 100% activity ( $k_{obs}$ ) was  $1.2 \times 10^{-2}$  s<sup>-1</sup>.

Addition		
Inhibitor (1.0 mM)	+ Metal ion (1.5 mM)	Enzyme activity (% of untreated enzyme)
PMSF	–	93.8
Thimerosal	–	27.5
Cysteine	–	29.2
	Zn <sup>2+</sup>	34.3
DTT	–	2.3
	Zn <sup>2+</sup>	2.0
1,10-Phenanthroline	–	0.0
EDTA	–	0.0
	Zn <sup>2+</sup>	90.8
	Co <sup>2+</sup>	99.6
	Mn <sup>2+</sup>	3.9
	Ca <sup>2+</sup>	0.7
DEPC (5 mM)	–	1.0*
+Fua-LGPA (150 mM)	–	12.6*

to the serine protease inhibitor PMSF, while the complex-forming compounds 1,10-phenanthroline and EDTA caused complete inhibition, indicating that Php-B is most probably a metalloprotease. Strong inhibition by DTT and partial inhibition by cysteine and thimerosal indicate a role for thiol group(s) in enzymic activity. An alternative possibility, i.e. that these inhibitors might remove catalytic metal ions, can be excluded because their inhibitory effects, unlike that of EDTA, could not be reversed by the addition of metal ions (Table 3).

For identification of the metal ion that is required for the enzymic activity of Php-B, we added to the reaction mixture containing EDTA-inhibited enzyme the bivalent metal ions Zn<sup>2+</sup>, Mn<sup>2+</sup>, Co<sup>2+</sup> and Ca<sup>2+</sup>, which are known to be essential for various metalloproteases. The enzyme activity was restored by both Zn<sup>2+</sup> and Co<sup>2+</sup>, but not by Mn<sup>2+</sup> or Ca<sup>2+</sup> (Table 3). Thus Php-B is either a Zn<sup>2+</sup>- or a Co<sup>2+</sup>-dependent enzyme. This needs to be clarified with further experiments. However, since in all known

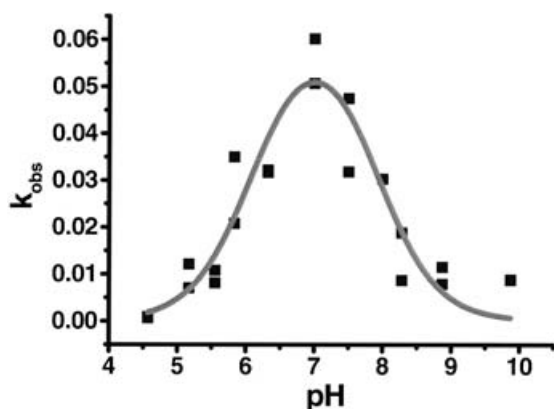


**Figure 3** pH-dependence of Fua-LGPA hydrolysis by Php-B

The final enzyme and Fua-LGPA concentrations in the reaction mixture were 13 nM and 73  $\mu$ M respectively. The time-dependence curves were fitted with Origin 5.0 software to obtain first-order rate constants ( $k_{obs}$ ). For the buffers used and other experimental conditions, as well as for the calculation of  $pK_a$  values, see the Experimental section.

$Co^{2+}$ -containing enzymes the  $Co^{2+}$  ion functions as a co-catalytic ion with  $Zn^{2+}$ , and in some of  $Zn^{2+}$ -dependent enzymes  $Zn^{2+}$  can be exchanged with  $Co^{2+}$  (e.g. the collagenase from *Clostridium histolyticum*), the more likely conclusion from our results is that Php-B is a  $Zn^{2+}$ -dependent metalloprotease.

Php-B exhibited maximal enzyme activity at pH 7.0 (Figure 3). Curve fitting to data points gave inflexion points at pH 6.1 ( $pK_{a1}$ ) and pH 7.9 ( $pK_{a2}$ ). The side-chain ionization constants that are the closest to these values are those of histidine (6.0) and cysteine (8.3) or an N-terminal amine (8.0–9.0). Since in most metalloproteases histidine residues take part in co-ordination of the catalytic metal ion, the involvement of histidine(s) in Php-B function is in good accordance with the enzyme's metalloprotease nature. This supposition is supported by the observation that DEPC, a reagent of histidine residues [29], abolished Php-B activity; in addition, this could be partially prevented if 1.5 mM substrate (Fua-LGPA) was present during DEPC treatment (Table 3). The value of  $pK_{a2}$ , if it is not a shifted ionization constant, suggests a role in Php-B function for a cysteine residue or an N-terminal amino group. The precise assignment of  $pK_{a2}$  to a particular group requires further investigation, but the sensitivity of Fua-LGPA hydrolysis to thiol reagents (Table 3) supports the involvement of cysteine residue(s).

### Php-B is likely to be a peptidase

The preference of Php-B for Fua-LGPA, a chromogen collagen peptide that is a quite selective synthetic substrate for bacterial collagenases and collagen peptidases [21], as well as the dependence of enzyme activity on  $Zn^{2+}$  ions, suggested that this protease might be a collagen-degrading enzyme of *P. luminescens*. However, when the enzyme activity was tested on two natural substrates, i.e. acid-soluble skin collagen type I and basal membrane collagen type IV, no cleavage was observed even after a 72 h incubation under conditions where these substrates were degraded within a few hours by *Clostridium histolyticum* collagenase (Sigma-Aldrich) (results not shown). Thus Php-B is not a true collagenase (these enzymes cleave native collagens such as types I and IV; see [14]). Php-B did not cleave denatured collagen (gelatin) or other non-collagen polypeptides, such as fibrinogen, casein and insulin B-chain, either (results not shown). The metal ion-dependent and thiol reagent-sensitive nature of Php-B, and its inability to hydrolyse large substrates, indicate that

this enzyme is a peptidase, similar to thimet oligopeptidases [30], and might have a role in the degradation of small, soluble collagen fragments.

To obtain further support for this assumption, we tested Php-B activity on three peptides in addition to those listed in Table 2, i.e. des-Arg<sup>1</sup>-bradykinin (a substrate cleaved at high rates by collagenolytic enzymes and collagen peptidases [28,31]), as well as P290 [(PPG)<sub>6</sub>] and P065 (KTEVSSVS), using the same enzyme/peptide ratio at which Fua-LGPA hydrolysis was measured. Similar to most of the peptides in Table 2, the activity of Php-B on peptides P065 and P290 was very poor: during a 1 h incubation, the cleavage of P065 was 45%, while P290 was not cleaved. In contrast, 90% of des-Arg<sup>1</sup>-bradykinin was cleaved within 5 min, indicating a reaction rate comparable with Fua-LGPA hydrolysis. The properties of Php-B, i.e. that it cannot cleave native or denatured collagen but readily hydrolyses des-Arg<sup>1</sup>-bradykinin and Fua-LGPA, are similar to those of a peptidase described from *Treponema denticola* [28]. On the basis of these properties, we propose that Php-B is a peptidase of *P. luminescens* that hydrolyses short collagen-derived peptides. Such a collagen peptidase enzyme in a pathogen may have a role in the bioconversion of host proteins during infection.

We thank A. Patthy for the peptides P065 and P290. This work was supported by a research grant (T037907) from OTKA (Hungary) to I. V.

### REFERENCES

- Boemare, N. E., Akhurst, R. J. and Mourant, R. G. (1993) DNA relatedness between *Xenorhabdus* spp. (Enterobacteriaceae), symbiotic bacteria of entomopathogenic nematodes, and a proposal to transfer *Xenorhabdus luminescens* to a new genus, *Photorhabdus* gen. nov. *Int. J. Syst. Bacteriol.* **43**, 249
- Szallas, E., Koch, C., Fodor, A., Burghardt, J., Buss, O., Szentirmai, A., Neelson, K. H. and Stackebrandt, E. (1997) Phylogenetic evidence for the taxonomic heterogeneity of *Photorhabdus luminescens*. *Int. J. Syst. Bacteriol.* **47**, 402–407
- Fischer-Le Saux, M., Viillard, V., Brunel, B., Normand, P. and Boemare, N. E. (1999) Polyphasic classification of the genus *Photorhabdus* and proposal of new taxa: *P. luminescens* subsp. *luminescens* subsp. nov., *P. luminescens* subsp. *akhurstii* subsp. nov., *P. luminescens* subsp. *laumondii* subsp. nov., *P. temperata* sp. nov., *P. temperata* subsp. *temperata* subsp. nov. and *P. asymbiotica* sp. nov. *Int. J. Syst. Bacteriol.* **49**, 1645–1656
- Forst, S., Dowds, B., Boemare, N. and Stackebrandt, E. (1997) *Xenorhabdus* and *Photorhabdus* spp.: bugs that kill bugs. *Annu. Rev. Microbiol.* **51**, 47–72
- Gaugler, R., Lewis, E. and Stuart, R. J. (1997) Ecology in the service of biological control: the case of entomopathogenic nematodes. *Oecologia* **109**, 483–489
- Dunphy, G. B. and Webster, J. M. (1988) Virulence mechanisms of *Heterorhabditis heliothidis* and its bacterial associate, *Xenorhabdus luminescens*, in non-immune larvae of the greater wax-moth, *Galleria melonella*. *Int. J. Parasitol.* **18**, 729–737
- Daborn, P. J., Waterfield, N., Blight, M. A. and ffrench-Constant, R. H. (2001) Measuring virulence factor expression by the pathogenic bacterium *Photorhabdus luminescens* in culture and during insect infection. *J. Bacteriol.* **183**, 5834–5839
- Bowen, D., Rocheleau, T. A., Blackburn, M., Andreev, O., Golubeva, E., Bhartiya, R. and ffrench-Constant, R. H. (1998) Insecticidal toxins from the bacterium *Photorhabdus luminescens*. *Science* **280**, 2129–2132
- Blackburn, M., Golubeva, E., Bowen, D. and ffrench-Constant, R. H. (1998) A novel insecticidal toxin from *Photorhabdus luminescens*, toxin complex A (Tca), and its histopathological effects on the midgut of *Manduca sexta*. *Appl. Environ. Microbiol.* **64**, 3036–3041
- Bowen, D. J. and Ensign, J. C. (1998) Purification and characterization of a high-molecular-weight insecticidal protein complex produced by the entomopathogenic bacterium *Photorhabdus luminescens*. *Appl. Environ. Microbiol.* **64**, 3029–3035
- Guo, L., Fatig, III, R. O., Orr, G. L., Schafer, B. W., Strickland, J. A., Sukhupinda, K., Woodsworth, A. T. and Petell, J. K. (1999) *Photorhabdus luminescens* W-14 insecticidal activity consists of at least two similar but distinct proteins. Purification and characterization of toxin A and toxin B. *J. Biol. Chem.* **274**, 9836–9842
- Dalhammar, G. and Steiner, H. (1984) Characterization of Inhibitor A, a protease from *Bacillus thuringiensis* which degrades attacins and cecropins, two classes of antibacterial proteins in insects. *Eur. J. Biochem.* **139**, 247–252

- 13 Flyg, C., Kenne, K. and Boman, H. G. (1980) Insect pathogenic properties of *Serratia marcescens*: phage-resistant mutants with a decreased resistance to *Cecropia* immunity and a decreased virulence to *Drosophila*. *J. Gen. Microbiol.* **120**, 173–181
- 14 Harrington, D. J. (1996) Bacterial collagenases and collagen-degrading enzymes and their potential role in human disease. *Infect. Immun.* **64**, 1885–1891
- 15 Bleakley, B. H. and Neelson, K. (1988) Characterization of primary and secondary forms of *Xenorhabdus luminescens* strain Hm. *FEMS Microbiol. Ecol.* **53**, 241–246
- 16 Schmidt, T. M., Bleakley, B. H. and Neelson, K. (1988) Characterization of an extracellular protease from an insect pathogen *Xenorhabdus luminescens*. *Appl. Environ. Microbiol.* **54**, 2793–2797
- 17 Wee, K. E., Yonan, C. R. and Chang, F. N. (2000) A new broad-spectrum protease inhibitor from the entomopathogenic bacterium *Photorhabdus luminescens*. *Microbiology* **146**, 3141–3147
- 18 Bowen, D., Blackburn, M., Rocheleau, T., Grutzmacher, C. and French-Constant, R. H. (2000) Secreted proteases from *Photorhabdus luminescens*: separation of the extracellular proteases from the insecticidal Tc toxin complexes. *Insect Biochem. Mol. Biol.* **30**, 69–74
- 19 Schechter, I. and Berger, A. (1967) On the size of the active site in proteases. I. Papain. *Biochem. Biophys. Res. Commun.* **27**, 157–162
- 20 Holmquist, B., Bunning, P. and Riordan, J. F. (1979) A continuous spectrophotometric assay for angiotensin converting enzyme. *Anal. Biochem.* **95**, 540–548
- 21 Van Wart, H. E. and Steinbrink, D. R. (1981) A continuous spectrophotometric assay for *Clostridium histolyticum* collagenase. *Anal. Biochem.* **113**, 356–365
- 22 Barshop, B. A., Wrenn, R. F. and Frieden, C. (1983) Analysis of numerical methods for computer simulation of kinetic processes: development of KINSIM – a flexible, portable system. *Anal. Biochem.* **130**, 134–145
- 23 Zimmerle, C. T. and Frieden, C. (1989) Analysis of progress curves by simulations generated by numerical integration. *Biochem. J.* **258**, 381–387
- 24 Koerber, S. C. and Fink, A. L. (1987) The analysis of enzyme progress curves by numerical differentiation, including competitive product inhibition and enzyme reactivation. *Anal. Biochem.* **165**, 75–87
- 25 Graf, L., Jancso, A., Szilagyi, L., Hegyi, G., Pinter, K., Naray-Szabo, G., Hepp, J., Medzihradsky, K. and Rutter, W. J. (1988) Electrostatic complementarity within the substrate-binding pocket of trypsin. *Proc. Natl. Acad. Sci. U.S.A.* **85**, 4961–4965
- 26 Kaiser, E., Colescott, R. L., Bossinger, C. D. and Cook, P. I. (1970) Color test for detection of free terminal amino groups in the solid-phase synthesis of peptides. *Anal. Biochem.* **34**, 595–598
- 27 Feder, J. (1968) A spectrophotometric assay for neutral protease. *Biochem. Biophys. Res. Commun.* **32**, 326–332
- 28 Makinen, K. K., Makinen, P. L. and Syed, S. A. (1992) Purification and substrate specificity of an endopeptidase from the human oral spirochete *Treponema denticola* ATCC 35405, active on furylacryloyl-Leu-Gly-Pro-Ala and bradykinin. *J. Biol. Chem.* **267**, 14285–14293
- 29 Hegyi, G., Premecz, G., Sain, B. and Muhrad, A. (1974) Selective carbethoxylation of the histidine residues of actin by diethylpyrocarbonate. *Eur. J. Biochem.* **44**, 7–12
- 30 Barrett, J. A. and Chen, J.-M. (1998) Thimet oligopeptidase. In *Handbook of Proteolytic Enzymes* (Barrett, A. J., Rawlings, N. D. and Woessner, F. J., ed.), pp. 1106–1112, Academic Press, London
- 31 Makinen, K. K. and Makinen, P. L. (1987) Purification and properties of an extracellular collagenolytic protease produced by the human oral bacterium *Bacillus cereus* (strain Soc 67). *J. Biol. Chem.* **262**, 12488–12495

Received 24 July 2003/14 January 2004; accepted 26 January 2004

Published as BJ Immediate Publication 26 January 2004, DOI 10.1042/BJ20031116